https://doi.org/10.48048/tis.2022.1487

Effects of Carrier Heating on Raman Susceptibility of Weakly-Polar Semiconductor Magneto-Plasmas

Gopal[1,*], B. S. Sharma[1] and Manjeet Singh[2]

[1]*Department of Physics, Lords University, Rajasthan 301028, India*
[2]*Department of Physics, Government College, Haryana 124106, India*

([*]Corresponding author's e-mail: gopal.lordsuniv@gmail.com)

Received: 22 December 2021, Revised: 23 February 2022, Accepted: 2 March 2022, Published: 5 November 2022

Abstract

In this paper, we develop a mathematical model to study the effects of carrier heating induced by a laser beam on Raman susceptibility of weakly-polar semiconductor magneto-plasmas. Using coupled mode approach, we obtain expressions for the real and imaginary parts of Raman susceptibility ($Re(\chi_R)$,$Im(\chi_R)$) under hydrodynamic and rotating-wave approximations. In order to validate the results, we perform numerical analysis for n-InSb crystal - CO_2 laser system. We observed change of sign of $Re(\chi_R)$ as well as $Im(\chi_R)$ around resonances. The carrier heating induced by the intense laser beam modifies the momentum transfer collision frequency of plasma carriers and consequently the Raman susceptibility of the semiconductor magneto-plasma, which subsequently enhances $Re(\chi_R)$ and $Im(\chi_R)$, (ii) shifts the enhanced $Re(\chi_R)$ and $Im(\chi_R)$ towards smaller values of applied magnetic field, and (iii) broadens the applied magnetic field regime at which change of sign of $Re(\chi_R)$ and $Im(\chi_R)$ are observed. The analysis leads to better understanding of Raman nonlinearity of semiconductor plasma and suggests an idea of development of Raman nonlinearity based optoelectronic devices.

Keywords: Carrier heating, Raman susceptibility, Stimulated Raman scattering, Semiconductors-plasmas, Magnetic field, Doping concentration

Introduction

The nonlinear optical susceptibility may be regarded as the most important parameter that characterizes the nonlinear optical response of a medium. It characterizes the overall response of nonlinear optical devices. In general, it is a complex quantity. Its real and imaginary parts are responsible for the nonlinear absorption and nonlinear index of refraction, respectively [1]. The change of sign of real and imaginary parts of nonlinear optical susceptibility exhibits various nonlinear optical processes [2]. The selection of a nonlinear optical medium, its operating frequency, mode generation, and mode scattering are regarded as the important features for the development of nonlinear optical devices.

Among the rich variety of nonlinear optical media, semiconductors, especially doped $A^{III}B^{V}$ type semiconductors, offer enhanced flexibility for development of nonlinear optical devices [3]. When exposed to laser beam, various coherent modes are generated. Some important modes include the plasmon mode (arises due to carrier density perturbations), the acoustical phonon mode (arises due to lattice vibrations), the optical phonon mode (arises due to molecular vibrations) etc. The scattering of laser beam from these modes lead to important nonlinear optical processes. Among the various nonlinear optical processes, the study of stimulated Raman scattering (SRS) is continuing a broad field of research owing to its important applications in modern optics [4-6]. SRS is caused by scattering of a laser beam by optical phonon mode in a nonlinear medium. Various aspects of SRS in semiconductors have been studied by the knowledge of Raman susceptibility by several research groups [7,8]. Recently, free and bound charge carriers contribution on real and imaginary parts of Raman susceptibility in weakly-polar magnetoactive semiconductors has been studied by Singh *et al.* [9]. Imaginary part of Raman susceptibility has been used to study steady-state and transient Raman amplification coefficients of semiconductor magneto-plasmas for possible applications in development of Raman amplifiers by Gopal *et al.* [10]. Therefore, the study of characteristic dependence of Raman susceptibility on various affecting factors is important from the fundamental as well as application viewpoints. One such factor is the carrier heating induced by intense laser beam. The influence of carrier heating induced by intense laser beam on

the real and imaginary parts of Raman susceptibility of semiconductors is not found in the available literature.

In this paper, we develop a mathematical model to study the effects of carrier heating induced by a laser beam on real and imaginary parts of Raman susceptibility of weakly-polar semiconductor magneto-plasmas under hydrodynamic and rotating-wave approximations. The motivation for this study originated from the fact that the carrier heating induced by the laser beam may remarkably modify the nonlinearity of the nonlinear optical medium, consequently the real and imaginary parts of Raman susceptibility, and subsequently the SRS based nonlinear optical processes. This study also leads to better understanding of SRS processes in semiconductor magneto-plasmas. In order to validate the results, we perform mathematical calculations for n-InSb crystal - CO_2 laser system chosen as a representative weakly-polar semiconductor - laser system.

Materials and methods

In order to obtain expressions for the real and imaginary parts of Raman susceptibility ($Re(\chi_R)$ and $Im(\chi_R)$), we consider an n-type doped weakly-polar semiconductor subjected to an external magnetic field represented by $\vec{B}_0 = \hat{z}B_0$. Such a semiconductor medium may be treated as rich of plasma carriers (here electrons) and is known as weakly-polar semiconductor magneto-plasma. In order to excite SRS, we consider the irradiation of semiconductor magneto-plasma by an infrared (pump) laser radiation field represented by$E_0(x,t) = E_0\, exp[\, i(k_0 x - \omega_0 t)]$. As a consequence of the laser-semiconductor nonlinear interaction, a coherent optical phonon mode represented by $u(x,t) = u_0\, exp[\, i(k_{op}x - \omega_{op}t)]$ is generated in the semiconductor magneto-plasma. This coherent optical phonon mode scatters the laser radiation field at Stokes shifted component represented by $E_s(x,t) = E_s\, exp[\, i(k_s x - \omega_s t)]$. These field are inter-linked via phase matching constraints: $\hbar(\omega_0, \vec{k}_0) = \hbar(\omega_{op}, \vec{k}_{op}) + \hbar(\omega_s, \vec{k}_s)$, where $\hbar\omega_0$, $\hbar\omega_{op}$, $\hbar\omega_s$ and $\hbar\vec{k}_0$, $\hbar\vec{k}_{op}$, $\hbar\vec{k}_s$ represent the energy and momentum possessed by pump field, optical phonon mode, and scattered Stokes component of pump field, respectively. We employ the well-known hydrodynamic model (valid only in the limit $k_{op}.l \ll 1$; l being the mean free path of plasma carriers) under thermal equilibrium

The basic equations used in the formulation of $Re(\chi_R)$ and $Im(\chi_R)$ are:

$$\frac{\partial^2 u}{\partial t^2} + \Gamma\frac{\partial u}{\partial t} + \omega_{opo}^2 u = \frac{1}{M}(q_s E + 0.5\varepsilon\alpha_u \bar{E}^2(x,t)) \quad (1)$$

$$\frac{\partial \vec{v}_0}{\partial t} + \nu_0\vec{v}_0 = -\frac{e}{m}[\vec{E}_0 + (\vec{v}_0 \times \vec{B}_0)] = -\frac{e}{m}(\vec{E}_e) \quad (2)$$

$$\frac{\partial \vec{v}_1}{\partial t} + \nu_0\vec{v}_1 + \left(\vec{v}_0.\frac{\partial}{\partial x}\right)\vec{v}_1 = -\frac{e}{m}[\vec{E}_1 + (\vec{v}_1 \times \vec{B}_0)] \quad (3)$$

$$\frac{\partial n_1}{\partial t} + n_0\frac{\partial v_1}{\partial x} + n_1\frac{\partial v_0}{\partial x} + v_0\frac{\partial n_1}{\partial x} = 0 \quad (4)$$

$$\vec{P}_{mv} = \varepsilon N\alpha_u u^*\vec{E}_e \quad (5)$$

$$\frac{\partial E_{1s}}{\partial x} + \frac{1}{\varepsilon}\frac{\partial}{\partial x}(|\vec{P}_{mv}|) = -\frac{n_1 e}{\varepsilon}. \quad (6)$$

Eqs.(1) - (6) and the notations used are well explained in [7-9]. Here, N is the number of molecules (harmonic oscillators) per unit volume and M is the molecular weight. $\Gamma \approx 10^{-2}\omega_{opo}$; where Γ is the damping constant (taken to be equal to phenomenological phonon-collision frequency) and ω_{opo} is the un-damped optical phonon mode frequency (taken to be equal to longitudinal optical phonon mode frequency). $\bar{E} = \frac{e}{m}(|\vec{E}_e|)$; where m is the mass and e is the charge of a plasma carrier. q_s represents the Szigeti effective charge and $\alpha_u = (\partial\alpha/\partial u)_0$ stand for the differential polarizability. $\vec{v}_0$ (n_0) and $\vec{v}_1$ (n_1) are respectively the equilibrium and perturbed oscillatory fluid velocities (plasma carriers concentration), respectively. ν_0 represents the momentum transfer collision frequency (MTCF) of plasma carriers. $\vec{P}_{mv}$ represents the molecular vibrational polarization. E_{1s} represents the space charge field. $\varepsilon = \varepsilon_0\varepsilon_\infty$; ε_0 and $\varepsilon_\infty$are the absolute and high frequencies permittivities of weakly-polar semiconductor magneto-plasma, respectively.

From Eq. (2), we obtain the *x*- and *y*-components of equilibrium fluid velocity of plasma carriers as:

$$v_{0x} = \frac{e(\nu+i\omega_0)}{m(\omega_c^2-\omega_0^2+2i\nu\omega_0)}E_0, \tag{7a}$$

and

$$v_{0y} = \frac{\omega_c}{(\nu+i\omega_0)}v_{0x}, \tag{7b}$$

where $\omega_c = \frac{eB_0}{m}$ is the cyclotron frequency.

From Eq. (3), we obtain the *x*- and *y*-components of perturbed fluid velocity of plasma carriers as:

$$v_{1x} = \frac{\nu}{(\nu^2+\omega_c^2)}\left[\bar{E} - ik_0\left(\frac{k_BT_0}{mn_0}\right)n_1\right], \tag{8a}$$

and

$$v_{1y} = \frac{\omega_c}{(\nu^2+\omega_c^2)}\left[-\bar{E} + ik_0\left(\frac{k_BT_0}{mn_0}\right)n_1\right], \tag{8b}$$

where k_B is the Boltzmann's constant andT_0 is the temperature of semiconductor magneto-plasma.

For exciting SRS, we consider the illumination of weakly-polar semiconductor magneto-plasma by an intense infrared laser radiation. The plasma carriers gain energy from the laser radiation field and consequently they attain a temperature T_e (i.e. carrier heating) somewhat higher than the temperature (T_0) of the semiconductor magneto-plasma. Subsequently, the MTCF of plasma carriers, which was ν_0 in the absence of carrier heating, turns to ν in the presence of carrier heating. The MTCF in the presence and absence of carrier heating are related as [11]:

$$\nu = \nu_0\left(\frac{T_e}{T_0}\right)^{1/2}. \tag{9}$$

We determine the ratio T_e/T_0 via the concept of conservation of energy under steady-state condition. Following the method adopted by Sodha*et al.* [12] and using Eqs. (7a) - (7b), the time independent component of power gained by the plasma carriers from laser radiation field is obtained as:

$$\frac{e}{2}Re(\vec{v}_{0x}.\vec{E}_e^*) = \frac{e^2\nu_0}{2m}\frac{(\omega_c^2-\omega_0^2)}{[(\omega_c^2-\omega_0^2)^2+4\nu_0^2\omega_0^2]}\left|\vec{E}_0\right|^2, \tag{10}$$

where $Re(\vec{v}_{0x}.\vec{E}_e^*)$ stands for the real part of $(\vec{v}_{0x}.\vec{E}_e^*)$.

Following the method adopted by Conwell [13], the power loss by plasma carriers during their collisions with polar optical phonons (POPs) is obtained as:

$$\left(\frac{\partial\in}{\partial t}\right)_{diss} = eE_{po}(x_0)^{1/2}\kappa_0\left(\frac{2k_B\theta_D}{m\pi}\right)^{1/2}\left(\frac{x_e}{2}\right).exp\left(\frac{x_e}{2}\right).\frac{exp(x_0-x_e)-1}{exp(x_0)-1}, \tag{11}$$

where $x_0 = \frac{\hbar\omega_l}{k_BT_0}$ and $x_e = \frac{\hbar\omega_l}{k_BT_e}$, in which $\hbar\omega_l$ represents the energy of POPs and it may be expressed as: $\hbar\omega_l = k_B\theta_D$, where θ_D is the Debye temperature. $E_{po} = \frac{me\hbar\omega_l}{\hbar^2}\left(\frac{1}{\varepsilon_\infty}-\frac{1}{\varepsilon}\right)$ stands for the POPs scattering potential field.

Under steady-state condition, the power gained by the plasma carriers from the laser radiation field is equal to the power loss by plasma carriers during their collision with POPs. Using Eqs. (10) - (11) and a mathematical calculation yields:

$$\frac{T_e}{T_0} = 1 + \frac{e^2\nu_0(\omega_c^2-\omega_0^2)|\vec{E}_0|^2}{2m\omega_0^2[(\omega_c^2-\omega_0^2)^2+4\nu_0^2\omega_0^2]} \times \left[eE_{po}\kappa_0\left(\frac{2k_B\theta_D}{m\pi}\right)^{1/2}\left(\frac{x_0}{2}\right)\frac{(x_0)^{1/2}\,exp(x_0/2)}{exp(x_0)-1}\right]^{-1}, \tag{12}$$

Substitution of T_e/T_0 from Eq. (12) into Eq. (9) yields the modified MTCF as:

$$\nu \approx \nu_0 \left(1 + \frac{e^2 \nu_0 (\omega_c^2 - \omega_0^2) |\vec{E}_0|^2}{4m\omega_0^2[(\omega_c^2 - \omega_0^2)^2 + 4\nu_0^2\omega_0^2]} \times \left[eE_{po}\kappa_0 \left(\frac{2k_B\theta_D}{m\pi}\right)^{1/2} \left(\frac{x_0}{2}\right) \frac{(x_0)^{1/2} exp(x_0/2)}{exp(x_0) - 1}\right]^{-1}\right). \quad (13)$$

In the presence of laser radiation field, the internally generated molecular vibrations (at optical phonon mode frequency ω_{op}) changes the dielectric constant of the semiconductor magneto-plasma which lead to an energy exchange among the coherent electromagnetic fields differing in frequency by multiples of ω_{op} (i.e., $\omega_0 \pm p\omega_{op}$, where p = 1, 2, 3, …). The modes at sum and difference frequencies are known as anti-Stokes and Stokes modes, respectively. In SRS, the anti-Stokes modes are very much less intense in comparison to Stokes modes and hence they are neglected. Moreover, the higher-order Stokes modes (with $p \geq 2$) are of too much decreasing intensity and are also neglected. Thus, only the first-order Stokes mode (with p = 1) of the scattered component of intense laser radiation field needs to be considered.

Following the procedure adopted by Singh *et al.* [7], and using Eqs. (1) - (6), an expression for the perturbed plasma carrier concentration (n_{1op}) at optical phonon mode frequency (ω_{op}) of the weakly-polar semiconductor magneto-plasma is obtained as:

$$n_{1op} = \frac{2iMk_{op}(\omega_t^2 - \omega_{op}^2 + i\Gamma\omega_{op}) - \varepsilon N}{e\alpha_u E_0^*} \left(\frac{2q_s\alpha_u}{\varepsilon} - \alpha_u^2 |E_0|^2\right) u^*. \quad (14)$$

The perturbed plasma carrier concentration at optical phonon mode frequency beats the laser radiation field and yields fast component of plasma carrier concentration. Following the procedure adopted by Singh *etal.* [7], and using Eqs. (1) - (6), an expression for the fast component of perturbed plasma carrier concentration (n_{1s}) at first-order Stokes mode frequency (ω_s) of the weakly-polar semiconductor magneto-plasma is obtained as:

$$n_{1s} = \frac{ie(k_0 - k_{op})E_0}{m(\bar{\omega}_r^2 - \omega_s^2 - i\nu\omega_s)} n_{1op}^*. \quad (15)$$

In Eq. (15), $\bar{\omega}_r^2 = \omega_r^2 \left(\frac{\nu^2 - \omega_c^2}{\nu^2 + \omega_c^2}\right)$, where $\omega_r^2 = \frac{\omega_p^2 \omega_l^2}{\omega_t^2}$, in which $\omega_p = \left(\frac{n_0 e^2}{m\varepsilon}\right)^{1/2}$ represents the plasma frequency. $\omega_l = \frac{k_B\theta_D}{\hbar}$ represents the frequency of longitudinal component of optical phonon mode.

The nonlinear current density (at first-order Stokes mode frequencyω_s), including the effects of carrier heating induced by an intense laser radiation field, may be expressed as [7]:

$$J_{cd}(\omega_s) = n_{1s}^* e v_{0x}, \quad (16a)$$

which yields

$$J_{cd}(\omega_s) = \frac{\varepsilon k_{op}(k_0 - k_{op})|\bar{E}_0|^2 E_1}{(\bar{\omega}_r^2 - \omega_s^2 + i\nu\omega_s)(\nu - i\omega_s)} \times \left[1 - \frac{\varepsilon N}{2M(\omega_{rop}^2 + i\Gamma\omega_{op})} \left(\frac{2q_s\alpha_u}{\varepsilon} - \alpha_u^2 |E_0|^2\right)\right], \quad (16b)$$

where $\omega_{rop}^2 = \bar{\omega}_r^2 - \omega_{op}^2$.

The nonlinear induced polarization of the weakly-polar semiconductor magneto-plasma, including the effects of carrier heating induced by an intense laser radiation field, may be expressed as [7]:

$$P_{cd}(\omega_s) = \int J_{cd}(\omega_s) dt = \frac{-J_{cd}(\omega_s)}{i\omega_s}, \quad (17a)$$

which yields

$$P_{cd}(\omega_s) = \frac{\varepsilon_\infty e^2 k_{op}(k_0 - k_{op})|\bar{E}_0|^2 E_1}{m^2\omega_0\omega_s(\bar{\omega}_r^2 - \omega_s^2 + i\nu\omega_s)} \times \left[1 - \frac{\varepsilon N}{2M(\omega_{rop}^2 + i\Gamma\omega_{op})} \left(\frac{2q_s\alpha_u}{\varepsilon} - \alpha_u^2 |E_0|^2\right)\right]. \quad (17b)$$

Here, it should be mentioning that the weakly-polar semiconductor magneto-plasma also possesses a polarization $P_{mv}(\omega_s)$ originating via nonlinear interaction between internal generated molecular vibrational mode and intense laser radiation field. Using Eqs. (1) - (5) and a mathematical calculation

yields

$$P_{mv}(\omega_s) = \frac{\varepsilon^2\omega_0^2 N\alpha_u}{2M(\omega_c^2+i\Gamma\omega_{op})}|E_0|^2E_1. \quad (18)$$

Using Eqs. (17b) - (18), the effective nonlinear induced polarization of the weakly-polar semiconductor magneto-plasma, including the effects of carrier heating induced by an intense laser radiation field, is obtained as:

$$P(\omega_s) = P_{cd}(\omega_s) + P_{mv}(\omega_s),$$

which yields

$$P(\omega_s) = \frac{\varepsilon^2\omega_0^2 N\alpha_u|E_0|^2E_1}{2M(\omega_c^2+i\Gamma\omega_{op})} + \frac{\varepsilon_\infty e^2 k_{op}(k_0-k_{op})|\bar{E}_0|^2E_1}{m^2\omega_0\omega_s(\bar{\omega}_r^2-\omega_s^2+i\nu\omega_s)} \times \left[1 - \frac{\varepsilon N}{2M(\omega_{rop}^2+i\Gamma\omega_{op})}\left(\frac{2q_s\alpha_u}{\varepsilon} - \alpha_u^2|E_0|^2\right)\right]. \quad (19)$$

We know that the component of effective nonlinear induced polarization $P(\omega_s)$, proportional to $|\bar{E}_0|^2E_1$ yields third-order (viz. Raman) susceptibility χ_R. Defining $P(\omega_s) = \varepsilon_0\chi_R|\bar{E}_0|^2E_1$, the expression for Raman susceptibility of the weakly-polar semiconductor magneto-plasma, including the effects of carrier heating induced by an intense laser radiation field, is obtained as:

$$\chi_R = \frac{\varepsilon_0\varepsilon_\infty^2\omega_0^2 N\alpha_u}{2M(\omega_c^2+i\Gamma\omega_{op})} + \frac{\varepsilon_\infty e^2 k_{op}(k_0-k_{op})}{\varepsilon_0 m^2\omega_0\omega_s(\bar{\omega}_r^2-\omega_s^2+i\nu\omega_s)} \times \left[1 - \frac{\varepsilon N}{2M(\omega_{rop}^2+i\Gamma\omega_{op})}\left(\frac{2q_s\alpha_u}{\varepsilon} - \alpha_u^2|E_0|^2\right)\right]. \quad (20a)$$

Eq. (20) reveals that χ_R is a complex quantity and it can be represented as: $\chi_R = Re(\chi_R) + i\,Im(\chi_R)$, where $Re(\chi_R)$ and $Im(\chi_R)$ stand for the real and imaginary parts of complex χ_R. Rationalizing Eq. (20), we obtain

$$Re(\chi_R) = \frac{\varepsilon_0\varepsilon_\infty^2\omega_0^2\omega_c^2 N\alpha_u}{2M(\omega_c^4+\Gamma^2\omega_{op}^2)} + \frac{\varepsilon_\infty e^2 k_{op}(k_0-k_{op})(\bar{\omega}_r^2-\omega_s^2)}{\varepsilon_0 m^2\omega_0\omega_s[(\bar{\omega}_r^2-\omega_s^2)^2+\nu^2\omega_s^2)]} \times \left[1 - \frac{\varepsilon N\omega_{rop}^2}{2M(\omega_{rop}^2+\Gamma^2\omega_{op}^2)}\left(\frac{2q_s\alpha_u}{\varepsilon} - \alpha_u^2|E_0|^2\right)\right] \quad (20b)$$

$$Im(\chi_R) = \frac{\varepsilon_0\varepsilon_\infty^2\omega_0^2 N\alpha_u\Gamma\omega_{op}}{2M(\omega_c^4+\Gamma^2\omega_{op}^2)} + \frac{\varepsilon_\infty e^2\nu\omega_s k_{op}(k_0-k_{op})}{\varepsilon_0 m^2\omega_0\omega_s[(\bar{\omega}_r^2-\omega_s^2)^2+\nu^2\omega_s^2)]} \times \left[1 - \frac{\varepsilon N\Gamma\omega_{op}}{2M(\omega_{rop}^4+\Gamma^2\omega_{op}^2)}\left(\frac{2q_s\alpha_u}{\varepsilon} - \alpha_u^2|E_0|^2\right)\right]. \quad (20c)$$

Eqs. (20b) - (20c) illustrate that both $Re(\chi_R)$ and $Im(\chi_R)$ are influenced by Szigeti effective charge q_s, differential polarizability α_u, plasma carrier concentration n_0 (via plasma frequency ω_p), applied magnetic field B_0 (via cyclotron frequency ω_c), and laser field intensity I. It should be noted that $Re(\chi_R)$ and $Im(\chi_R)$ responsible for nonlinear refractive index and nonlinear absorption coefficient of the weakly-polar semiconductor plasma medium. Further, the knowledge of nonlinear refractive index and nonlinear absorption coefficient provide the information regarding the design of various nonlinear optical devices including amplifiers, oscillators, filters, and couplers. In the forthcoming section, Eqs. (20b) - (20c) are used for detailed analysis.

Results and discussion

In order to validate the results, we perform mathematical calculations for n-InSb crystal - CO_2 laser system chosen as a representative weakly-polar semiconductor - laser system. In n-type InSb crystal, electrons may be treated as the plasma carriers. The other material parameters of the representative sample are given in **Table 1** [6,7].

Table 1 Materihral parameters of n-InSb crystal at liquid nitrogen temperature.

Parameter	Value
Density, ρ (kg·m^{-3})	5.8×10^3
Electron's effective mass, m	$0.014m_0$
Molecular mass, M (kg)	2.7×10^{-29}

Parameter	Value
Number of molecules/volume (m^{-3})	1.48×10^{28}
Szigeti effective charge, q_s (coulomb)	1.2×10^{-20}
Differential polarizability, α_u (SI units)	0.068
Static dielectric constant, ε	15.8
High frequency dielectric constant, ε_∞	15.68
Debye temperature, θ_D (K)	278
Momentum transfer collision frequency, ν_0 (s^{-1})	3.5×10^{11}
Optical phonon mode frequency, ω_{op} (s^{-1})	3.7×10^{13}
Laser (pump) wave frequency, ω_0 (s^{-1})	1.78×10^{14}

Eqs. (20b) - (20c) represent $Re(\chi_R)$ and $Im(\chi_R)$ of the weakly-polar semiconductor magneto-plasma with including the effects of carrier heating induced by an intense laser radiation field. The expressions for $Re(\chi_R)$ and $Im(\chi_R)$ of the weakly-polar semiconductor magneto-plasma with excluding the effects of carrier heating induced by an intense laser radiation field can be obtained by simply replacing ν by ν_0 (at $T_e = T_0$) in these equations. The dependence of $Re(\chi_R)$ and $Im(\chi_R)$ on applied magnetic field B_0 (via cyclotron frequency ω_c) and doping concentration n_0 (via plasma frequency ω_p) with excluding and including the effects of carrier heating induced by an intense laser radiation field are explored. We targeted our aim:

(i) to find out the suitable values of applied magnetic field and doping concentration to enhance the real and imaginary parts of Raman susceptibility;

(ii) to search the importance of nonlinear optical devices based on Raman nonlinearities.

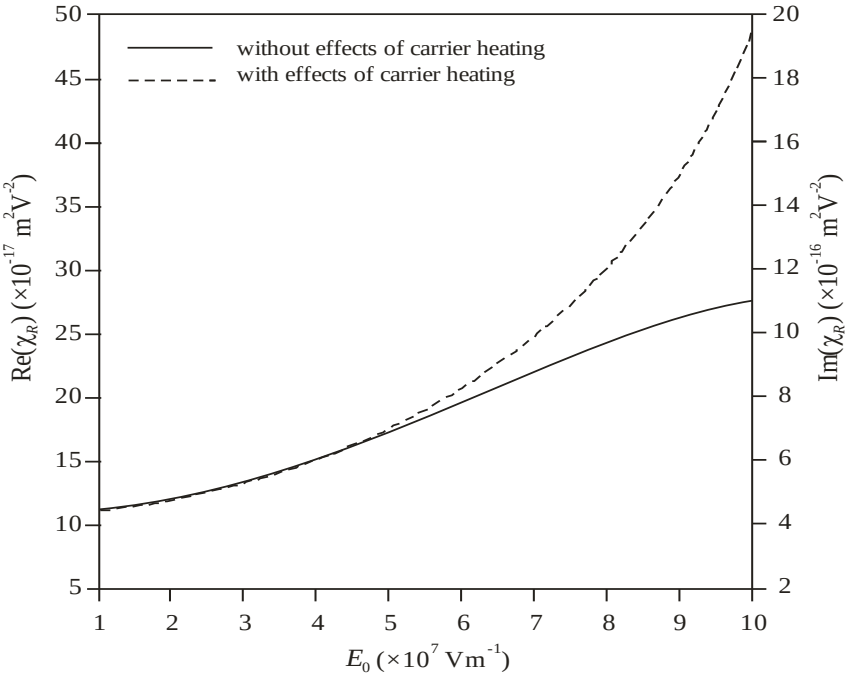

Figure 1 Nature of dependence of real and imaginary parts of Raman susceptibility ($Re(\chi_R)$,$Im(\chi_R)$) on pump amplitude (E_0) for the cases: (i) without effects of carrier heating, and (ii) with effects of carrier heating. Here $n_0 = 2.0 \times 10^{23}\text{m}^{-3}$ and $B_0 = 14.2\text{T}$.

Figure 1 shows the nature of dependence of real and imaginary parts of Raman susceptibility ($Re(\chi_R)$,$Im(\chi_R)$) on pump amplitude (E_0) for the cases: (i) without effects of carrier heating, and (ii) with effects of carrier heating. For either one of these cases, both $Re(\chi_R)$ and $Im(\chi_R)$ exhibit identical behavior towards pump amplitude; only the difference being that their magnitudes are slightly different. On comparing $Re(\chi_R)$ and $Im(\chi_R)$, the following ratio is obtained:

$$\frac{Re(\chi_R)}{Im(\chi_R)} = 0.25.$$

For pump amplitudes$E_0 < 4 \times 10^7 \mathrm{Vm}^{-1}$, both $Re(\chi_R)$ and $Im(\chi_R)$ exhibitthe parabolic variation and the curves corresponding to cases: (i) without effects of carrier heating, and (ii) with effects of carrier heating, coincide exactly. This suggests that the effects of carrier heating are insignificant for $E_0 < 4 \times 10^7 \mathrm{Vm}^{-1}$. However, at $E_0 = 4 \times 10^7 \mathrm{Vm}^{-1}$, the curves start deviating, indicating that the effects of carrier heating originated. The curve corresponding to case (i) depictsthe linear variation while the curve corresponding to case (ii) depicts the parabolic variation. With increasing pump amplitude beyond 4×10^7 Vm^{-1}, the separation between the curves increases, indicating that the effects of carrier heating are more pronounced at higher pump amplitudes. Around $E_0 \approx 10^8 \mathrm{Vm}^{-1}$, both $Re(\chi_R)$ and $Im(\chi_R)$ become almost double in the presence of carrier heating in comparison to theabsence of carrier heating.This behavior can be easily understood in terms of the temperature dependence of $Re(\chi_R)$ and $Im(\chi_R)$ on modified MTCF of plasma carriers in Eqs. (20b) - (20c). Here, it should be worth pointing out that Kumari *et al.* [14] studied the phenomenon of stimulated Brillouin scatteringin semiconductor magneto-plasmas and observed that for pump amplitudes $E_0 > 4 \times 10^7 \mathrm{Vm}^{-1}$, hot carrier effects on Brillouin susceptibility become significant and more pronounced at larger values of pump amplitudes. In the present study, the deviation of real and imaginary parts of Raman susceptibility, from their usual parabolic shape, emphasizes the necessity of incorporating the effects of carrier heating (at high pump amplitudes) in stimulated Raman scattering processes.

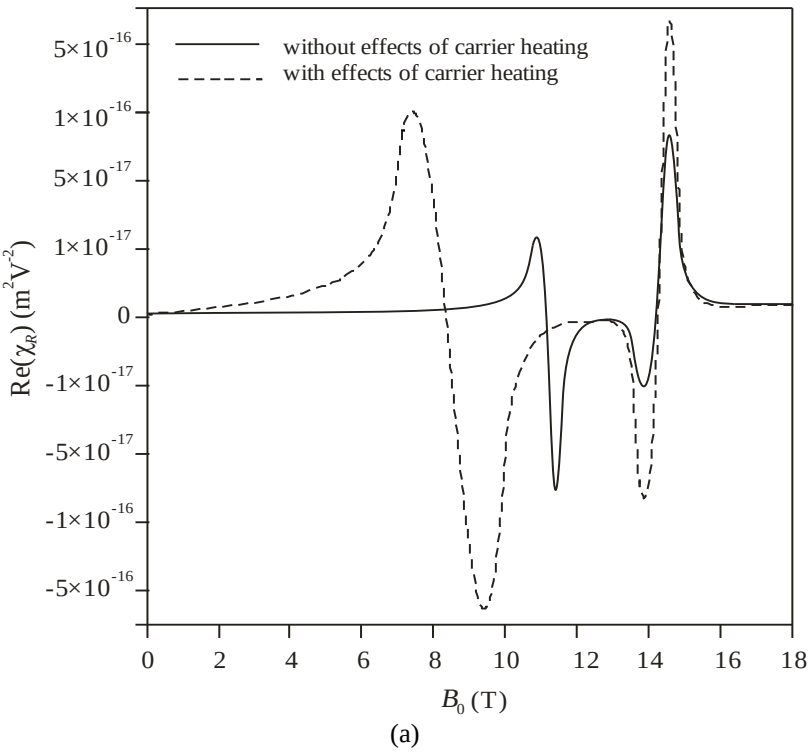

(a)

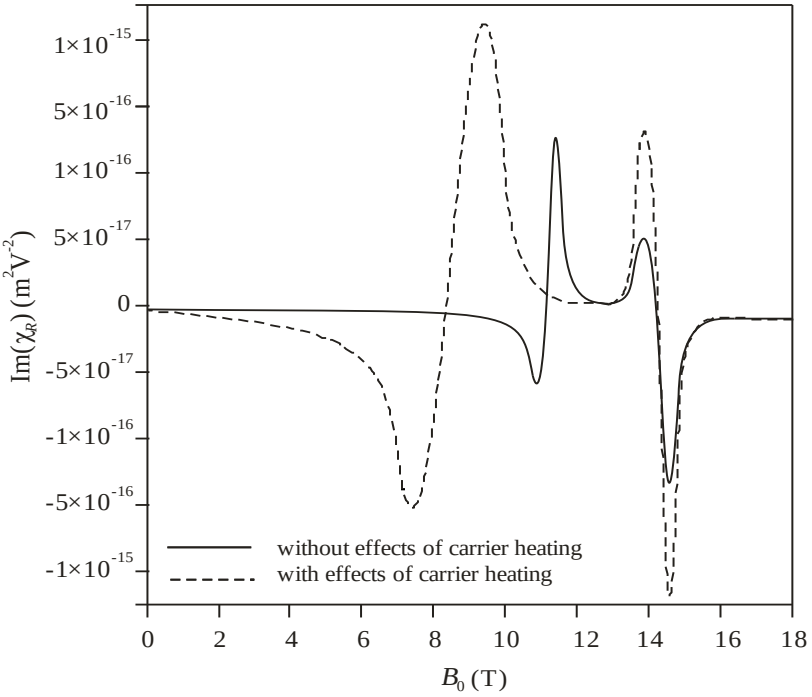

(b)

Figure 2 (a) Variation of real part of Raman susceptibility ($Re(\chi_R)$), and (b) Variation of imaginary part of Raman susceptibility ($Im(\chi_R)$) with applied magnetic field (B_0) for the cases: (i) without effects of carrier heating, and (ii) with effects of carrier heating. Here $n_0 = 2.0 \times 10^{23}\text{m}^{-3}$ and $E_0 = 6.8 \times 10^7\text{Vm}^{-1}$

Figures 2(a) -2(b) displays the variation of real and imaginary parts of Raman susceptibility ($Re(\chi_R)$,$Im(\chi_R)$) with applied magnetic field (B_0), respectively for the cases (i) without effects of carrier heating, and (ii) with effects of carrier heating. These clearly demonstrates the enhancement as well as change of sign of $Re(\chi_R)$ and$Im(\chi_R)$. A comparison between the nature of curves obtained in these figures clearly illustrate that the curves corresponding to $Re(\chi_R)$ and $Im(\chi_R)$ are exactly mirror images about the reference line.

When the effects of carrier heating are excluded, with increasing applied magnetic field, $Re(\chi_R)$ is positive while $Im(\chi_R)$ is negative, vanishingly small, and remain independent of applied magnetic field for$0 \leq B_0 \leq 8T$. With increasing applied magnetic field beyond this regime, $Re(\chi_R)$ starts increasing while $Im(\chi_R)$ starts decreasing attaining peak positive and negative values ($Re(\chi_R) = 2 \times 10^{-17}\text{m}^2\text{V}^{-2}$, $Im(\chi_R) = -6 \times 10^{-17}\text{m}^2\text{V}^{-2}$), respectively sharply at $B_0 = 10.44\text{T}$. With slightly increasing applied magnetic field beyond this value, $Re(\chi_R)$ starts decreasing while $Im(\chi_R)$ starts increasing very sharply. At $B_0 = 10.55\text{T}$, both $Re(\chi_R)$ and $Im(\chi_R)$ vanish simultaneously. With increasing applied magnetic field beyond this value, the real and imaginary parts of Raman susceptibility change their sign; $Re(\chi_R)$ becomes negative while $Im(\chi_R)$ becomes positive. The phenomenon of change of sign of $Re(\chi_R)$ and $Im(\chi_R)$ is known as 'dielectric anomaly'. With slightly increasing applied magnetic field beyond $B_0 = 10.55\text{T}$, $Re(\chi_R)$ starts decreasing while $Im(\chi_R)$ starts increasing attaining peak negative and positive values ($Re(\chi_R) = -7.5 \times 10^{-17}\text{m}^2\text{V}^{-2}$, $Im(\chi_R) = 2.5 \times 10^{-16}\text{m}^2\text{V}^{-2}$), respectively sharply at $B_0 = 10.72\text{T}$. With further increasing applied magnetic field beyond this value, $Re(\chi_R)$ starts increasing (but remains negative) while $Im(\chi_R)$ starts decreasing (but remains positive) very sharply, both become negligibly small around $B_0 \approx 13\text{T}$. This behaviour of $Re(\chi_R)$ and $Im(\chi_R)$ may be attributed to resonance between coupled cyclotron-plasmon frequency and Stokes mode frequency, i.e.$\bar{\omega}_r^2 \sim \omega_s^2$. The coupled cyclotron-plasmon mode frequency may be varied over desired regime by properly selecting either 1 or both the cyclotron frequency (via applied magnetic field) and plasmon frequency (via plasma carrier concentration). Accordingly, the scattered Stokes mode frequency may be tuned with coupled cyclotron-plasmon mode frequency to achieve resonance.

With increasing applied magnetic field beyond $B_0 \approx 13\text{T}$, $Re(\chi_R)$ starts decreasing while $Im(\chi_R)$

starts increasing attaining peak negative and positive values ($Re(\chi_R) = -1 \times 10^{-17}\text{m}^2\text{V}^{-2}$, $Im(\chi_R) = +5 \times 10^{-17}\text{m}^2\text{V}^{-2}$), respectively sharply at $B_0 = 13.8\text{T}$. With slightly increasing applied magnetic field beyond this value, $Re(\chi_R)$ starts increasing while $Im(\chi_R)$ starts decreasing very sharply. At $B_0 = 14.2\text{T}$, both $Re(\chi_R)$ and $Im(\chi_R)$ vanish simultaneously. With increasing applied magnetic field beyond this value, the real and imaginary parts of Raman susceptibility change their sign; $Re(\chi_R)$ becomes positive while $Im(\chi_R)$ becomes negative. With slightly increasing applied magnetic field beyond $B_0 = 14.2\text{T}$, $Re(\chi_R)$ starts increasing while $Im(\chi_R)$ starts decreasing attaining peak positive and negative values ($Re(\chi_R) = 8 \times 10^{-17}\text{m}^2\text{V}^{-2}$, $Im(\chi_R) = -3 \times 10^{-16}\text{m}^2\text{V}^{-2}$), respectively sharply at $B_0 = 14.4\text{T}$. With further increasing applied magnetic field beyond this value, $Re(\chi_R)$ starts decreasing (but remains positive) while $Im(\chi_R)$ starts increasing (but remains negative) very sharply, both become negligibly small even at higher values of applied magnetic field. This behaviour of $Re(\chi_R)$ and $Im(\chi_R)$ may be attributed to resonance between cyclotron frequency and pump wave frequency, i.e.$\omega_c^2 \sim \omega_0^2$.

When the effects of carrier heating are included, the features of $Re(\chi_R) - B_0$ and $Im(\chi_R) - B_0$ plots remain unchanged except that:

1) the change of sign of $Re(\chi_R)$ and $Im(\chi_R)$ which was taking place at $B_0 = 10.55\text{T}$ (excluding effects of carrier heating) is now shifted to $B_0 = 8.16\text{T}$;

2) the peak positive and negative values of $Re(\chi_R)$ and $Im(\chi_R)$ occurring due to resonance condition $\bar{\omega}_r^2 \sim \omega_s^2$ is now enhanced by approximately 1 order of magnitude;

3) the range of applied magnetic field at which dielectric anomaly of $Re(\chi_R)$ and $Im(\chi_R)$ due to resonance condition $\bar{\omega}_r^2 \sim \omega_s^2$ was occurring is now widened; and

4) the peak positive and negative values of $Re(\chi_R)$ and $Im(\chi_R)$ occurring due to resonance condition $\omega_c^2 \sim \omega_0^2$is now enhanced by more than 1 order of magnitude; without shifting and widening on the applied magnetic field axis.

An important aspect of the result obtained in **Figures 2(a)** and **(2b)** is to control and to obtain enhanced values of the real and imaginary parts of Raman susceptibility via proper selection of applied magnetic field in semiconductor magneto-plasmas. The results also permit the tuning of scattered Stokes mode over a broad frequency regime and reveal the opportunity of fabrication of frequency converters.

In **Figures 3(a)** and **3(b)**, real part of Raman susceptibility ($Re(\chi_R)$) is plotted versus applied magnetic field (B_0) for 3 different values of plasma carrier concentration ($n_0 = 2.0 \times 10^{23}$, $2.1 \times 10^{23}$and $2.2 \times 10^{23}\text{m}^{-3}$) for the cases: (i) without effects of carrier heating, and (ii) with effects of carrier heating, respectively. These figures depict the enhancement as well as dielectric anomaly of $Re(\chi_R)$ in semiconductor magneto-plasmas. For a given plasma carrier concentration (say $n_0 = 2.0 \times 10^{23}\text{m}^{-3}$), the nature of curves are similar to that drawn in **Figure 2(a)**. With increasing plasma carrier concentration (say $n_0 = 2.1 \times 10^{23}$or $2.2 \times 10^{23}\text{m}^{-3}$), the magnitude of peak (positive and negative) value of $Re(\chi_R)$ remains constant; the values of applied magnetic field at which change of sign of $Re(\chi_R)$ occurring due to resonance condition $\bar{\omega}_r^2 \sim \omega_s^2$ is shifted towards smaller values. The curves corresponding to different values of n_0 meet at $B_0 \approx 13\text{T}$ and thereafter they exhibit common behaviour with respect to applied magnetic field, independent of plasma carrier concentration. Comparing the nature of curves obtained in **Figures 3(a)** and **3(b)** reveal that for a selected value of plasma carrier concentration, the inclusion of effects of carrier heating causes widening of the magnetic field regime at which dielectric anomaly of $Re(\chi_R)$ occurs. The result of **Figures 3(a)** and **3(b)** support the results of **Figure 2(a)**.

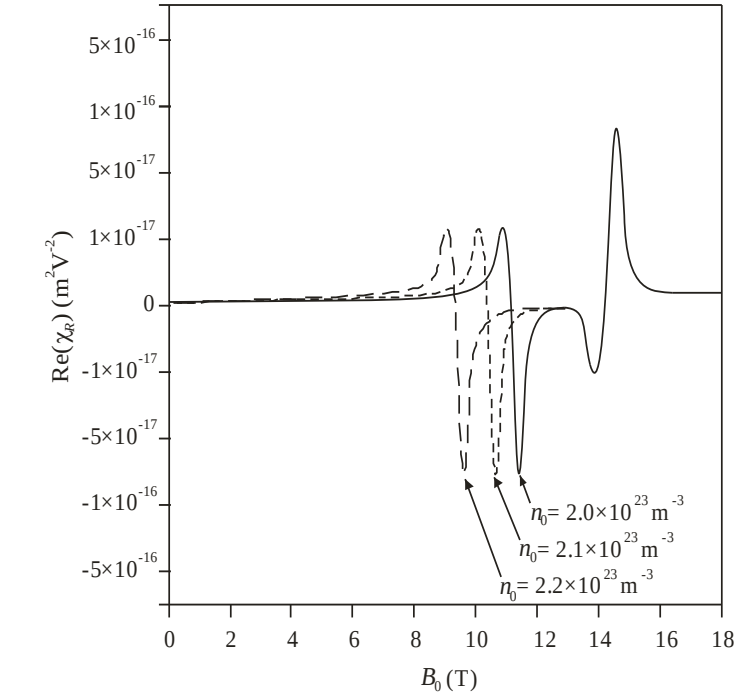

(a)

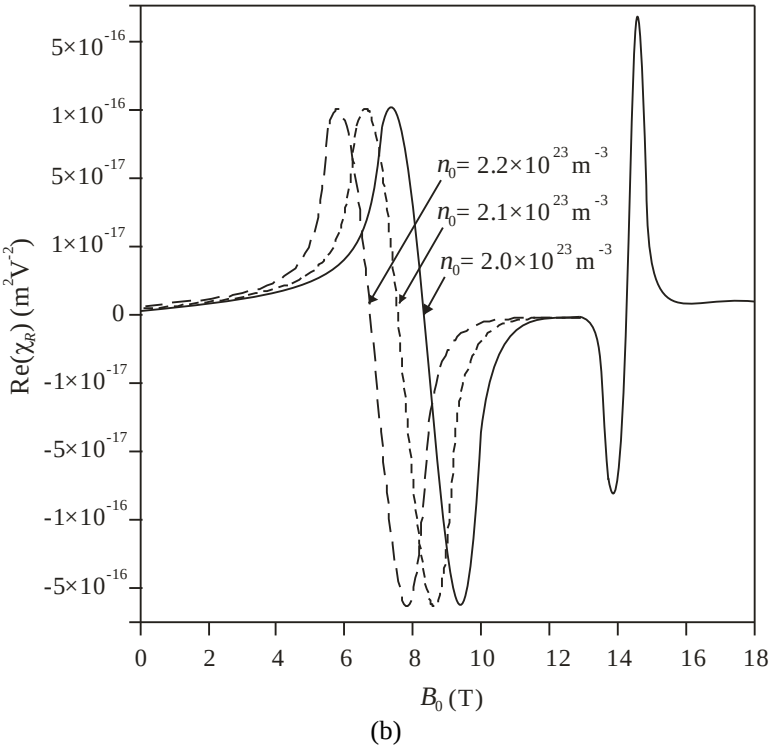

(b)

Figure 3 (a) and (b) Variation of real part of Raman susceptibility ($Re(\chi_R)$) with applied magnetic field (B_0) for 3 different values of plasma carrier concentration ($n_0 = 2.0 \times 10^{23}$, $2.1 \times 10^{23}$and $2.2 \times 10^{23}\mathrm{m}^{-3}$) with excluding the effects of carrier heating. Here $E_0 = 6.8 \times 10^7 \mathrm{Vm}^{-1}$.

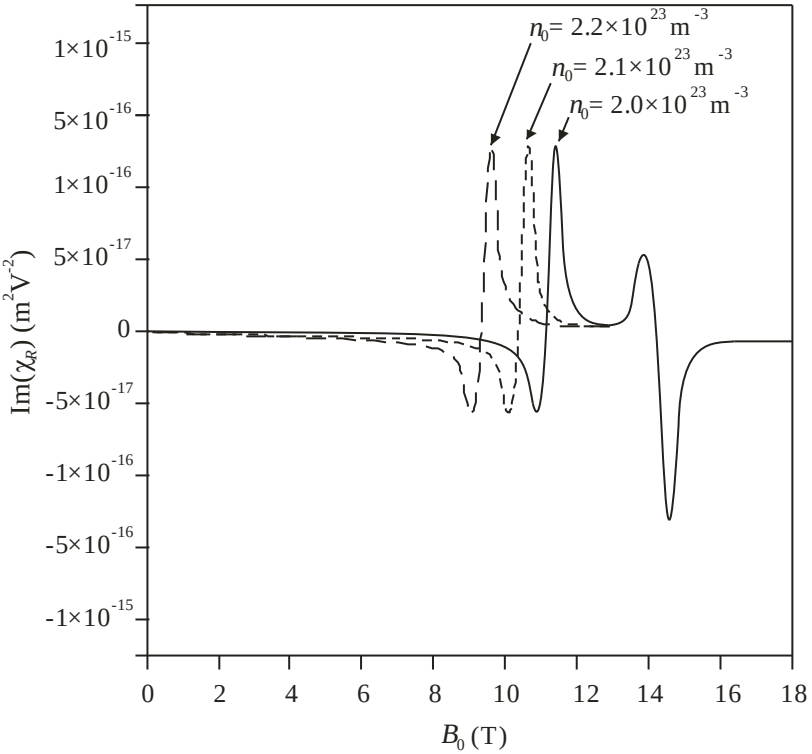

(a)

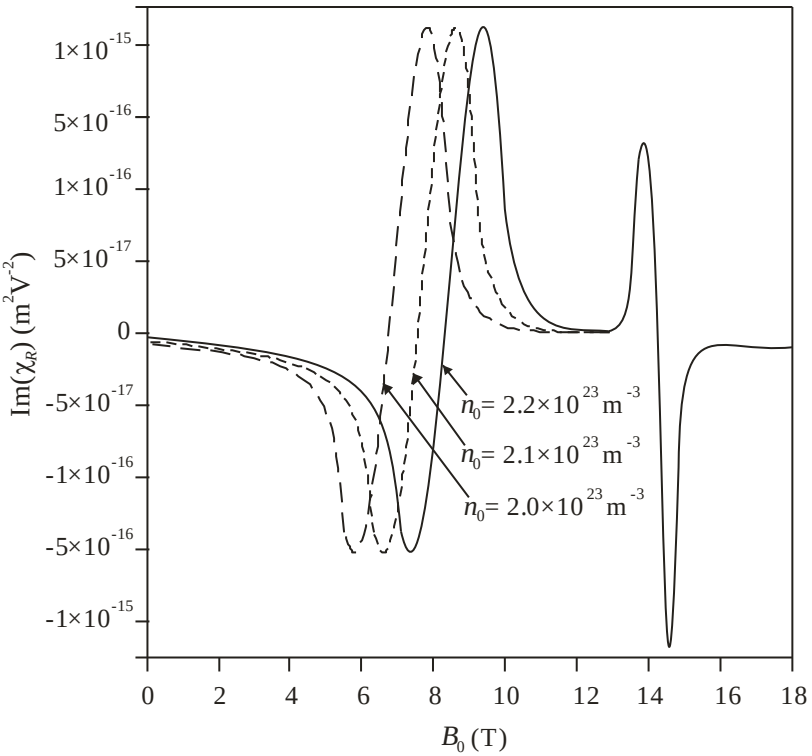

(b)

Figure 4 (a) and (b) Variation of imaginary part of Raman susceptibility ($Im(\chi_R)$) with applied magnetic field (B_0) for 3 different values of plasma carrier concentration ($n_0 = 2.0 \times 10^{23}$, $2.1 \times 10^{23}$and 2.2×10^{23}m^{-3}) with excluding the effects of carrier heating. Here $E_0 = 6.8 \times 10^7$Vm^{-1}.

In **Figures 4(a)** and **(4b)**, the imaginary part of Raman susceptibility ($Im(\chi_R)$) is plotted versus applied magnetic field (B_0) for 3 different values of plasma carrier concentration ($n_0 = 2.0 \times 10^{23}$, $2.1 \times 10^{23}$and 2.2×10^{23}m^{-3}) for the cases: (i) without effects of carrier heating, and (ii) with effects of carrier heating, respectively. These figures depict the enhancement as well as dielectric anomaly of $Im(\chi_R)$ in semiconductor magneto-plasmas. For a given plasma carrier concentration (say $n_0 = 2.0 \times 10^{23}$m^{-3}), the nature of curves are similar to that drawn in **Figure 2(b)**. With increasing plasma carrier concentration (say $n_0 = 2.1 \times 10^{23}$or 2.2×10^{23}m^{-3}), the magnitude of peak (positive and negative) value of $Im(\chi_R)$ remains constant; the values of applied magnetic field at which change of sign of $Im(\chi_R)$ occurring due to resonance condition $\bar{\omega}_r^2 \sim \omega_s^2$ is shifted towards smaller values. The curves corresponding to different values of n_0 meet at $B_0 \approx 13$T and thereafter they exhibit common behaviour with respect to applied magnetic field, independent of plasma carrier concentration. Comparing the nature of curves obtained in **Figures 4(a)** and **4(b)** reveal that for a selected value of plasma carrier concentration, the inclusion of effects of carrier heating causes widening of the magnetic field regime at which dielectric anomaly of $Im(\chi_R)$ occurs. The result of **Figures 4(a)** and **4(b)** support the results of **Figure 2(b)**.

The nature of dependence of real and imaginary parts of Raman susceptibility on applied magnetic field with excluding the effects of carrier heating depicted in **Figures 2**and **3** is well in agreement with results reported by Singh *et al.* [9]. However, the dependence of real and imaginary parts of Raman susceptibility on applied magnetic field with including the effects of carrier heating is not available in literature and first reported here. The relevant experiment has not been performed.

Conclusions

In this paper, the effects of carrier heating induced by a laser beam on Raman susceptibility of weakly-polar semiconductor magneto-plasmas are analyzed by the mathematical model and numerical analysis performed for n-InSb/CO_2 laser system. The analysis offers a tunable (viz., $\bar{\omega}_r^2 \sim \omega_s^2$) and a non-tunable (viz., $\omega_c^2 \sim \omega_0^2$) resonance condition. Both the resonance conditions causes dielectric anomaly of real as well as imaginary parts of Raman susceptibility. The carrier heating induced by the intense laser beam changes the momentum transfer collision frequency of plasma carriers and consequently the Raman susceptibility of the semiconductor magneto-plasma, which subsequently enhances $Re(\chi_R)$ and $Im(\chi_R)$, (ii) shifts the enhanced $Re(\chi_R)$ and $Im(\chi_R)$ towards smaller values of applied magnetic field, and (iii) broadens the applied magnetic field regime at which change of sign of $Re(\chi_R)$ and $Im(\chi_R)$ due to tunable resonance condition are observed. For pump amplitude $E_0 < 4 \times 10^7$Vm^{-1}, the effects of carrier heating on $Re(\chi_R)$ and $Im(\chi_R)$ are absent. However, for $E_0 \geq 4 \times 10^7$Vm^{-1}, the effects of carrier heating become significant and more pronounced at higher values of pump amplitude. The analysis leads to better understanding of Raman nonlinearity of semiconductor plasma and suggests an idea of development of Raman nonlinearity based optoelectronic devices such as optical switches and frequency converters.

Acknowledgements

The authors are very thankful to Prof. Sib Krishna Ghoshal, Department of Physics, Universiti Teknologi, Malaysia for many useful suggestions to carry out this work and careful reading of the final draft.

References

[1] M Singh, P Aghamkar, N Kishore and PK Sen. Nonlinear absorption and refractive index of Brillouin scattered mode in semiconductor-plasmas by an applied magnetic field. *Optic. Laser Tech*. 2008; **40**, 215-22.

[2] M Singh, J Gahlawat, A Sangwan, N Singh and M Singh. *Nonlinear optical susceptibilities of a piezoelectric semiconductor magneto-plasma*. *In*: VK Jain, S Rattan and A Verma (Eds.). Recent trends in materials and devices. Springer, Singapore, 2020, p.189-201.

[3] S Mokkapati and C Jagadish. III-V compound SC for optoelectronic devices. *Mater. Today* 2009; **12**, 22-32.

[4] MNIslam. Raman amplifiers for telecommunications. *IEEE J. Sel. Top. Quant. Electron*. 2002; **8**, 548-59.

[5] VV Yakovlev, GI Petrov, HF Zhang, GD Noojin, ML Denton, RJ Thomas and MO Scully. Stimulated Raman scattering: Old physics, new applications. *J. Mod. Optic*. 2009; **56**, 1970-3.

[6] Q Cheng, Y Miao, J Wild, W Min and Y Yang. Emerging applications of stimulated Raman scattering microscopy in materials science. *Matter* 2021; **4**, 1460-83.
[7] J Singh, S Dahiya, A Kumarand M Singh. Enhanced Raman gain coefficients of semiconductor magneto-plasmas. *Optik* 2021; **248**, 168183.
[8] J Singh, S Dahiya and M Singh. Raman amplification in magnetoactive doped III-V semiconductors. *J. Optic*. 2022; **51**, 317-26.
[9] J Singh, S Dahiya and M Singh. Free and bound charge carriers dependent Raman susceptibilities in weakly-polar magnetoactive semiconductors. *Mater. Today Proc*. 2021; **46**, 5844-51.
[10] Gopal, BS Sharma, J Singh and M Singh. Steady-state and transient Raman gain coefficients of semiconductor magneto-plasmas (calculated for n-InSb-CO_2 laser system). *Iran. J. Sci. Tech. Trans. A Sci.* 2022; **46**, 697-708.
[11] AC Beer. *Galvanometric effects in semiconductors: Solid state physics*. Academic Press, New York, 1963.
[12] MS Sodha, AK Ghatak and VK Tripathi. *Self-focusing of laser beams in dielectrics, plasmas and semiconductors*. Tata McGraw, New Delhi, India, 1974, p. 55-62.
[13] EM Conwell. *High field transport in semiconductors*. Academic Press, New York, 1967, p. 159.
[14] P Kumari, BS Sharma and M Singh. Hot carrier effects on Brillouin susceptibilities of semiconductor magnetoplasmas. *Pramana J. Phys*. 2022; **96**, 49.